2004

Application of Pyrolysis-GC/MS for Rapid Assessment of Organic Contamination in Sediments from Barcelona Harbor

Michael A. Kruge
Montclair State University, krugem@mail.montclair.edu

Albert Permanyer
University of Barcelona

Application of Pyrolysis-GC/MS for Rapid Assessment of Organic Contamination in Sediments from Barcelona Harbor*

Michael A. Kruge[a], Albert Permanyer[b]

[a]*Department of Earth and Environmental Studies, Montclair State University, Montclair, New Jersey, USA*
[b]*Departament de Geoquímica, University of Barcelona, Barcelona, Catalonia, Spain*

Abstract

Pyrolysis-GC/MS is advantageous as a tool for rapid sediment contamination assessment because of the small sample size required, minimal sample preparation, and its ability to detect a wide variety of organic pollutants as well as naturally-occurring biological materials. Py-GC/MS was applied, together with determination of organic carbon, and major and minor element concentrations, to evaluate potentially contaminated sediments in the port of Barcelona (Spain) and the adjacent Llobregat River delta. Detected contaminant markers, most evident in the Old Port (*Port Vell*) area, included hopanes and alkylated PAHs (petroleum), sterenes (sewage), C_{16}-C_{19} phenylalkanes (detergents) and parent PAHs (combusted fuels).

1. Introduction

Waterways in the world's great port cities have been subject to many decades of environmental degradation, as an unintended consequence of shipping, industrial activity near the water's edge, and non-point urban discharge within the associated watershed. Harbor and coastal waters provide natural laboratories for the study of the impact of urban runoff, airfall combustion debris, shipping activities and navigational dredging. Organic substances form a significant fraction of the potential pollutants in these urban systems, often originating as fossil fuels (raw or modified) and the combustion products thereof. As such, analytical methods initially developed for petroleum exploration are well suited for organic pollution assessment in sediments.

Barcelona, a major port city of 1.6 million inhabitants, which in 2001 handled 132 MTn of total port traffic, is situated along the northwestern margin of the Mediterranean Sea (Fig. 1). The Port of Barcelona is currently undergoing major upgrades, therefore continuing environmental assessment is important. The first objective was to perform a preliminary study of Barcelona harbor sediment pollution to provide a baseline for further study after completion of the modifications to the port's facilities. A secondary objective was the testing

Figure 1. Location map showing a) Spain, b) Catalonia and c) the Barcelona harbor and Llobregat River area. Sampling transects with six sites each are shown. Triangle marks a major sewage treatment plant outfall north of the mouth of the Llobregat. Modified from base maps and airphotos produced by the Institut Cartogràfic de Catalunya, the Centre de Recerca Ecològica i Aplicacions Forestals (Barcelona) and the Diputació de Barcelona.
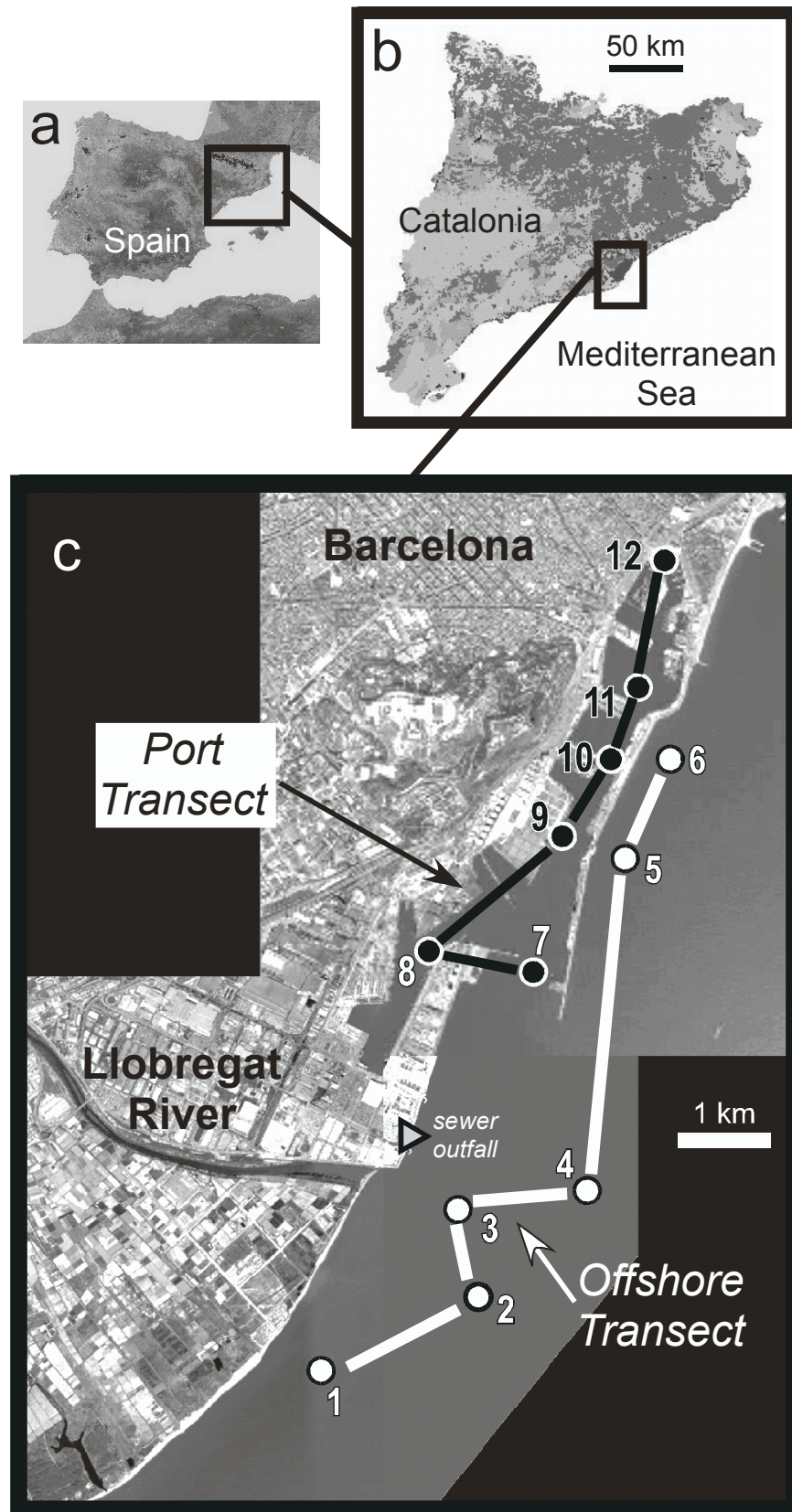
of Py-GC/MS as a means of screening for organic contaminants including petroleum, sewage and fossil fuel combustion products. An ultimate goal is the collection of a high resolution geochemical data set for incorporation in a geographic information system (GIS).

Pyrolysis-gas chromatography/mass spectrometry (Py-GC/MS) offers a practical alternative for rapid, inexpensive, semiquantitative molecular organic analysis, simply employing milligram quantities of dry, whole sediment. This solvent-free, microanalytic technique can be considered to be in the spirit of environmentally-benign "green chemistry". The compounds detected comprise an information-rich mixture of thermally extractable components and the products of the thermal decomposition of (bio)polymers present in the sample. The mass spectrometer may be operated in full-scan mode, appropriate for exploratory investigations, or in selected ion monitoring mode, for the routine detection of trace compounds suspected to be present. Pyrolysis-gas chromatographic and related methods have demonstrated their effectiveness as tools for molecular analysis in environmental studies (Richnow et al., 1995; Barrio et al., 1996; U.S.E.P.A., 1996; Abdel Bagi et al., 1996; Kruge et al., 1998; Kruge, 1999; Deshmukh et al., 2001; Mansuy et al., 2001; Faure et al., 2002; Jardé et al., 2003).

2. Methods

2.1. Samples

A series of 12 sediment grab samples (plus two replicates) were collected from Barcelona's port area, covering ca. 10 km of the coastal zone (Fig. 1, Table 1). Sampling sites 1-6 range offshore from the Llobregat River delta northeast along the outer margin of the harbor breakwater ("offshore transect"). Sediment sampling sites 7-12 are situated along the docks within the port ("port transect"). The replicate cores were taken at sites 10 and 12. The samples were collected using the procedures specified by the Spanish Centro de Estudios y Experimentación del Ministerio de Obras Públicas. At each site, samples were collected in triplicate using a 20 cm wide sampler similar to a Petite Ponar. Depth of penetration into the sediment was 5 to 10 cm. Samples were dried at ambient temperature and manually homogenized.

2.2. Elemental analysis

The raw, disaggregated, dry sediment was analyzed for total organic carbon (TOC) content using a Leco instrument. Elemental analyses were performed by Activation Laboratories, Ltd. of Ancaster (ON) Canada. Sulfur and phosphorus were determined by inductively coupled plasma optical emission spectroscopy (ICP-OES) and metals by inductively coupled plasma mass spectrometry (ICP-MS) following aqua regia extraction, except mercury, which was determined by an atomic absorption spectrophotometer (Table 1). U.S.G.S. analytical standards GXR-1, 2, 4 and 6 were employed.

Table 1. Sample identification, locations and results of elemental analyses. A value of 0 indicates that the results were below instrumental detection limits; nd: not determined.

Sample	Core	Location Description	UTM Coordinates (n East	North	Water Depth (m)	C org %	Al %	Ca %	Fe %	K %	Mg %	Na %	P %	S %	Ag μg/g	Cd μg/g	Cu μg/g	Mn μg/g	Mo μg/g	Ni μg/g	Pb μg/g	Zn μg/g	Cr μg/g	Hg ng/g	Pyrolysis-GC/MS full scan	SIM
1	B-541	Llobregat delta	428258	5E+06	10	0.01	0.29	10.16	0.89	0.05	0.87	0.41	0.020	0.08	0.0	0.0	3	205	0.0	7	16	54	8	42		X
2	B-542	Llobregat delta	429889	5E+06	15	0.33	0.51	13.11	1.58	0.11	1.12	0.74	0.026	0.26	0.0	0.0	26	284	5.6	14	24	100	12	112		X
3	B-543	Llobregat R. mouth (proxim:	429688	5E+06	10	0.92	0.64	11.42	1.71	0.13	0.90	1.05	0.053	0.27	1.0	0.5	48	304	0.5	21	31	141	35	178		X
4	B-544	Llobregat R. mouth (distal)	431032	5E+06	15	1.54	0.96	11.69	1.98	0.22	1.06	1.02	0.032	0.51	0.5	0.0	27	301	3.5	15	29	109	28	215		X
5	B-545	Breakwater (Moll Conten.)	431446	5E+06	20	0.91	0.87	7.20	2.28	0.20	0.80	0.62	0.050	0.28	1.9	0.6	68	381	5.5	21	125	350	108	880		X
6	B-546	Breakwater (new port mouth	431912	5E+06	20	0.22	0.68	8.44	1.51	0.18	0.59	0.44	0.027	0.16	0.2	0.5	25	305	5.9	9	71	155	26	213		X
7	B-547	Port mouth	430464	5E+06	16	0.76	0.85	9.35	1.83	0.20	0.91	0.80	0.031	0.47	1.3	2.7	65	312	5.8	21	116	322	85	1009	X	X
8	B-548	Fuels dock	429350	5E+06	12	0.17	0.27	2.54	0.43	0.06	0.27	0.42	0.011	0.09	0.3	0.7	9	72	3.1	5	11	80	9	56		X
9	B-549	Container dock	430767	5E+06	14	0.37	1.01	10.21	2.20	0.24	0.91	0.69	0.025	0.19	0.0	0.7	18	393	1.6	18	22	102	19	67		X
10	B-550	Inner breakwater	431245	5E+06	12	0.98	0.83	9.10	1.94	0.21	0.89	0.84	0.044	0.34	1.9	0.4	81	293	5.0	18	65	197	35	661		X
10B	B-553	Inner breakwater (replicate c	"	"	"	1.12	0.59	9.18	1.76	0.17	0.85	0.94	0.041	0.35	1.9	0.9	78	288	5.3	17	74	207	34	726		X
11	B-551	Moll Ponent-Moll Barcelon:	431574	5E+06	10	0.19	0.46	4.57	1.15	0.13	0.64	0.42	0.031	0.13	0.3	0.7	29	198	3.5	9	28	100	14	290		X
12	B-552	Old Port (Port Vell)	431854	5E+06	8	6.12	0.74	9.13	2.03	0.23	0.92	2.41	0.116	1.37	18.3	2.3	389	193	14.0	28	441	887	65	2985	X	X
12R	B-552	Old Port (repeat analysis)	"	"	"	nd	0.72	8.97	2.07	0.24	0.96	2.59	0.122	1.37	19.0	2.8	423	201	20.3	32	471	999	68	3062		
12B	B-554	Old Port (replicate core)	"	"	"	5.93	0.69	9.16	1.98	0.23	1.00	2.95	0.122	1.34	20.9	2.4	408	196	16.3	31	447	935	64	3157		X

Table 1

2.3. Pyrolysis-Gas Chromatography/Mass Spectrometry

Pyrolysis-gas chromatography/mass spectrometry (Py-GC/MS) was performed using a CDS 120 Pyroprobe, coupled to a HP 5890 gas chromatograph with a HP 5970 mass selective detector and a 50 m J&W Scientific DB-5MS column (0.2mm i.d., film thickness 0.33 μm). A measured amount (a few mg) of dry, powdered sample was pyrolyzed in a flow of helium for 20 sec. in a platinum coil at 600 °C, as measured by a thermocouple in the sample holder. The GC oven was operated under the following program: isothermal for 5 min at 40 °C; temperature programmed at 5 °C/min. to 300 °C and then isothermal for 30 min. The MS was operated in either full scan (50-450 Da, 1.21 scans/sec.) or selected ion monitoring (SIM) mode, 70eV ionization voltage. After performing full-scan Py-GC/MS on samples 7 and 12, the full suite of samples was analyzed with the mass spectrometer in selected ion monitoring (SIM) mode. The ions for the SIM mode (Table 2) were chosen based on study of the full scan results, to be sure that all major compounds are represented, as well as trace components such as PAHs and hopanes. The SIM approach improved sensitivity in detection of these target trace analytes, particularly in samples poor in organic matter.

2.4. Data processing

Quantification of Py-GC/MS data was accomplished using Hewlett Packard GC/MS software G1701AA (version A.03.00). Only SIM data were quantitated. All data were adjusted by response factors previously determined for each compound using this GC/MS instrument and normalized to the values for toluene in each sample. Toluene is a major pyrolysis product of many types of organic matter and is the most abundant compound in the pyrolyzate of every sediment sample in this study. The raw spectrometer counts for toluene (m/z 91), normalized to the weight of sediment pyrolyzed, were found to be proportional to the organic carbon concentrations in these samples (Fig. 2). The semiquantitative results for individual compounds presented herein may thus be considered to represent geochemically anomalous or "excess" quantities.

Absolute quantitation was not attempted using Py-GC/MS in this study. The consistent application of internal standards (e.g., decadeuteropyrene) has proven difficult. Therefore, in cases where absolute quantitation may be required, the Py-GC/MS approach is not recommended. On the other hand, relative quantitation described gives reproducible Py-GC/MS results that lead to useful geochemical insights.

Principal components analysis using organic carbon, major and trace element and Py-GC/MS data was performed using JMP version 5.0 software (SAS Institute Inc, 2002). The initial analysis employed 122 variables comprising the elemental data (Table 1) and the quantitated compounds determined by Py-GC/MS (Table 2), normalized to toluene. Examination of the results showed that many of the variables were closely correlated. For the subsequent analysis, therefore, the 122 variables were reduced to 34 compounds, elements and groupings of related compounds or elements, as a means of simplification (Table 3). The normalized data set was scaled by taking the square root of all values prior to the multivariate analysis.
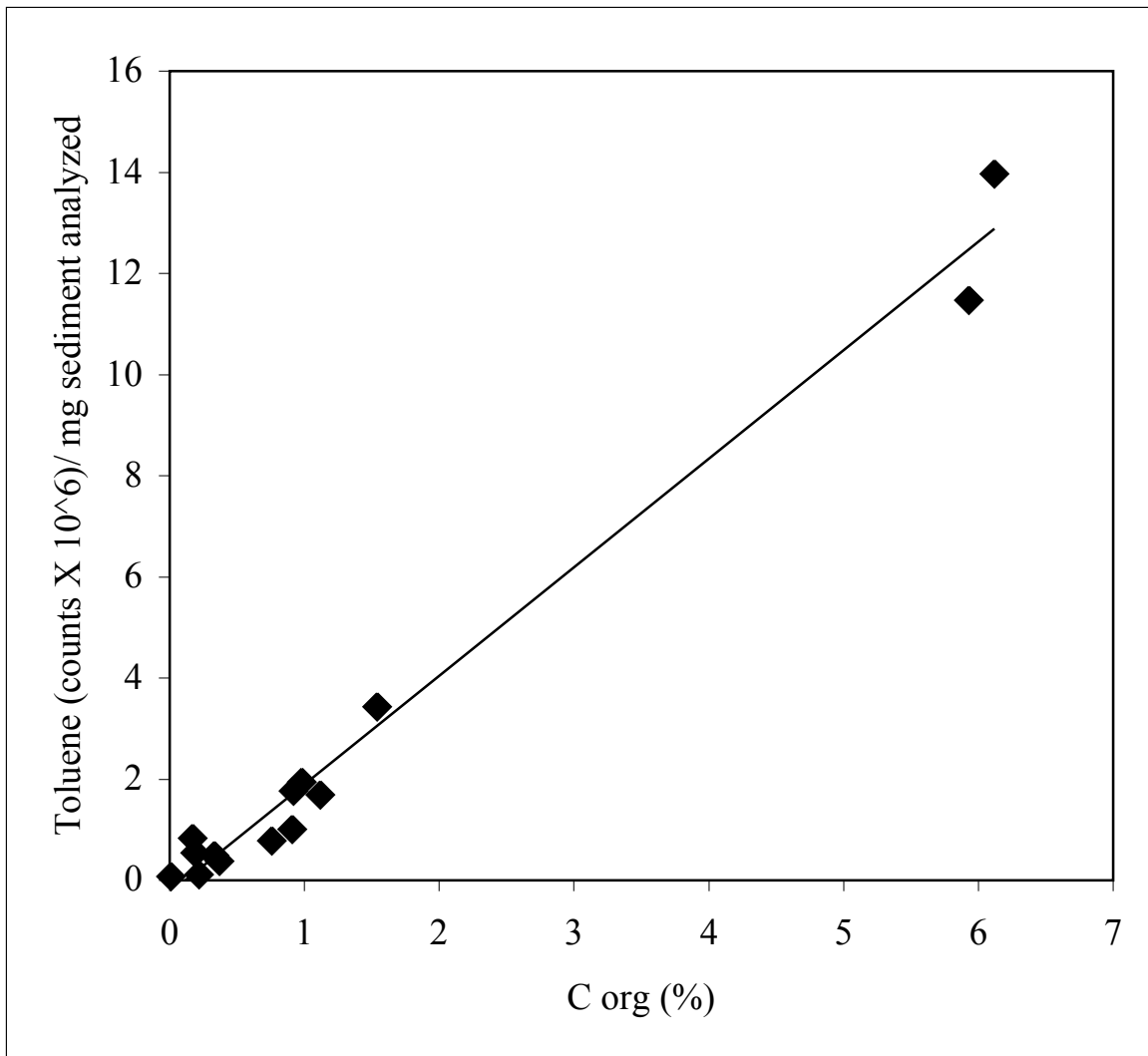
Figure 2. Plot showing the correspondence between organic carbon content and MS counts for toluene (m/z 91), normalized to the amount of sediment pyrolyzed. Trend line has r2 = 0.98.

Table 2. Chromatographic peak identification and listing of MS ions used in quantification of compounds detected by Py-GC/MS. NQ: not quantitated. The compound classes are keyed as follows - IS: isoprenoids, B: alkylbenzenes, PA: phenylalkanes, A2: diaromatic hydrocarbons, A3: triaromatic hydrocarbons, A4: tetraaromatic hydrocarbons, A5: pentaaromatic hydrocarbons, HO: hopanes, ST: steroid hydrocarbons, F: phenols, CA: carboxylic acids, PS: polysaccharide derivatives, T: sulfur compounds. The organonitrogen compound classes are PL: pyrroles, PD: pyridines, IL: indoles, AN: alkylnitriles, AM: alkylamides.

Peak	Compound	RT	m/z	Type	Peak	Compound	RT	m/z	Type
1	pyridine	11.78	79	PD	35	4-phenyltridecane	47.15	91	PA
2	pyrrole	11.86	67	PL	36	anthracene	47.16	178	A3
3	toluene	12.65	91	B	37	n-hexadecanitrile	48.28	69	AN
4	2-methylthiophene	12.84	97	T	38	3-methylphenanthrene	49.40	192	A3
5	1-methylthiophene	13.21	97	T	39	n-hexadecanoic acid	49.43	69	CA
	methylpyridine(a)	14.86	93	PD	40	2-methylphenanthrene	49.55	192	A3
	furancarboxaldehyde	15.49	95	PS		n-tetradecanamide	49.78	NQ	AM
	cyclopentenone	15.54	82	PS	41	methylanthracene	49.80	192	A3
6	2-methylpyrrole	15.64	80	PL	42	9-methylphenanthrene	49.98	192	A3
7	3-methylpyrrole	15.99	80	PL	43	1-methylphenanthrene	50.11	192	A3
8	ethylbenzene	16.76	NQ	B	44	phenyl naphthalene	50.88	NQ	A3
	methylpyridine(b)	16.90	93	PD	45	n-octadecanitrile	52.55	69	AN
9	styrene	18.21	104	B	46	1,7-dimethylphenanthrene	52.57	NQ	A3
	3-methylcyclopentenone	18.67	96	PS	47	dimethylphenanthrenes	52.57	206	A3
	C2-pyrrole	19.34	94	PL	48	fluoranthene	53.16	202	A4
	methylfurancarboxaldehyde	20.98	110	PS	49	methylphenylnaphthalene	53.42	NQ	A3
	2-methylcyclopentenone	21.16	96	PS	50	n-hexadecanamide	53.95	NQ	AM
10	phenol	21.57	94	F	51	pyrene	54.38	202	A4
11	2-methylphenol	24.44	107	F	52	retene	55.70	NQ	A3
12	4&3-methylphenols	25.23	107	F	53	benzo[a]fluorene	56.07	216	A4
	guaiacol	25.84	124	F	54	n-eicosanitrile	56.37	69	AN
	2,4-dimethylphenol	27.88	107	F	55	methylpyrene	56.42	216	A4
13	4-ethylphenol	28.47	107	F	56	2-methylpyrene	56.63	216	A4
14	naphthalene	29.76	128	A2	57	dimethylphenylnaphthalene	57.04	NQ	A3
	dihydrobenzofuran	30.25	120	PS?	58	4-methylpyrene	57.12	216	A4
15	indole	33.03	117	IL	59	1-methylpyrene	57.28	216	A4
16	2-methylnaphthalene	33.37	142	A2		n-octadecanamide	57.82	NQ	AM
17	1-methylnaphthalene	33.89	142	A2	60	n-doeicosanitrile	60.20	69	AN
18	methylindole	35.89	130	IL	61	benzo[a]anthracene	60.98	228	A4
	dimethylnaphthalenes	37.20	156	A2	62	chrysene	61.22	228	A4
19	5-phenyldecane	39.52	91	PA	63	3-methylchrysene	63.79	242	A4
20	4-phenyldecane	39.79	91	PA	64	2-methylchrysene	64.04	242	A4
	trimethylnaphthalenes	40.13	170	A2	65	6-methylchrysene	64.33	242	A4
21	6-phenylundecane	41.97	91	PA	66	1-methylchrysene	64.79	242	A4
22	5-phenylundecane	42.07	91	PA	67	cholestene	68.57	215	ST
23	4-phenylundecane	42.36	91	PA	68	benzo[j&k&b]fluoranthene	69.38	252	A5
24	C4-naphthalenes	43.00	NQ	A3	69	cholestene	69.40	NQ	ST
25	prist-1-ene	44.21	69	IS	70	cholestene	69.80	NQ	ST
26	6-phenyldodecane	44.38	91	PA	71	cholestene	70.40	215	ST
27	prist-2-ene	44.46	69	IS	72	cholestane	70.50	NQ	ST
28	5-phenyldodecane	44.49	91	PA	73	cholestene	70.71	215	ST
29	biphenyl	44.60	NQ	F	74	benzo[a]pyrene	72.15	252	A5
30	4-phenyldodecane	44.76	91	PA	75	benzo[e]pyrene	72.76	252	A5
31	dibenzothiophene	46.15	198	T	76	perylene	73.66	252	A5
32	6-phenyltridecane	46.65	91	PA	77	ethylcholestene	78.11	215	ST
33	5-phenyltridecane	46.82	91	PA	78	norhopane	79.97	191	HO
34	phenanthrene	46.88	178	A3	79	hopane	84.38	191	HO

Table 2

Table 3. Variables used the principal components analysis experiment illustrated in Figure 7, sorted by the eigenvector associated with the first principal component. See text sections 2.4 and 3.2.1 for explanation of variable selection.

Variable	Eigenvector (1st principal component)
Hg + Ag	0.261
organic carbon	0.256
phenylalkanes	0.247
sulfur	0.247
Cu + Pb + Zn	0.245
phosphorus	0.242
sodium	0.241
C2-alkylphenols	0.224
alkylamides	0.218
C16-C29 n-alkanes	0.217
polysaccharide derivatives	0.217
C27 + C29 sterenes	0.212
indoles	0.208
monoaromatic hydrocarbons	0.197
methylphenols	0.183
dimethylphenanthrenes + dimethylanthracenes	0.171
norhopane + hopane	0.164
alkylnitriles	0.113
C8-C15 n-alkanes	0.106
C3-alkylnaphthalenes	0.087
methylphenanthrenes + methylanthracenes	0.087
K + Al + Fe	0.086
C2-alkylnaphthalenes	0.051
pyrroles	0.038
chrysene + benzo[a]anthracene + methylchrysenes	0.001
Ca + Mg	-0.003
pyridines	-0.010
pyrene + fluoranthene + benzo[a]fluorene + methylpyrenes	-0.043
phenol	-0.063
methylnaphthalenes	-0.075
pentaaromatic hydrocarbons	-0.078
phenanthrene + anthracene	-0.128
thiophenes	-0.140
naphthalene	-0.235

Table 3

3. Results and Discussion

3.1. Consideration of the Old Port sediment (sampling site 12)

The sediment sample from the Old Port (*Port Vell*) is very distinctive, having by far the highest concentrations of lead (453 μg/g), mercury (3068 ng/g), as well as silver, copper, zinc and other trace metal pollutants in the sample set (Table 1). These high concentrations indicate that the site (Fig. 1) has been severely impacted by urban/industrial contamination, not unsurprising since it is situated at the centuries-old heart of the city. It is also anomalously enriched in organic carbon (6 %), sulfur and phosphorus, indicating that it is also in receipt of organic pollution, the nature of which must be determined by molecular means (see below). The high C_{org}, S and P concentrations suggest that the water column above has been experiencing local hypoxia, not unexpected since water circulation is likely to be impeded by the breakwater (Fig. 1).

The total ion pyrogram produced from sediment sample 12 (Fig. 3a) features prominent peaks of the simple monoaromatic hydrocarbons toluene and styrene [3, 9] and simple phenols [10, 12], which are common in the pyrolyzates of most types of recent sedimentary organic matter (e.g., Sicre et al., 1994; Peulvé et al., 1996; Kruge et al., 1998) and are not very diagnostic. (Numbers in square brackets refer to peak numbers in the figures and Table 2.) More interestingly, indole [15] is also relatively abundant and closer examination reveals the presence of other simple organonitrogen compounds, including pyrroles, pyridines and methylindole [1, 2, 6, 7, 18]. These are characteristic pyrolysis products of proteins and degraded proteinaceous matter in sediments (Sicre et al., 1994; Peulvé et al., 1996; Garcette-Lepecq et al., 2000; Zang and Hatcher, 2002) and signal the presence of algal and/or bacterial organic matter, in this case, fairly abundant. This interpretation is compatible with the suspected incidences of hypoxia inferred from the elevated C_{org}, S and P concentrations mentioned above.

The pronounced baseline hump maximizing near the elution time of the C_{24} *n*-alkane (Fig. 3a) is due to a chromatographically unresolved complex mixture of compounds likely to be thermally-desorbed biodegraded petroleum or fuel oil. The presence of relatively abundant, thermally-desorbed petroleum hopanes [78,79], usually resistant to biodegradation (Peters and Moldowan, 1993), strongly supports this conclusion. C_{27} and C_{29} sterenes and steranes [67, 69-73, 77] are remarkably abundant in the pyrolyzate. The sterenes in particular are likely to derive from recent organic matter, rather than petroleum, possibly produced by high temperature alteration in the pyrolyzer from cholesterol (Rushdi et al., 2003) and other biological steroids present in the sediment. Sewage in the sediment would be the most likely source of the steroids; several researchers have documented the presence of geochemical tracers for sewage in the environment near Barcelona (Palanques, 1994; Palanques and Diaz, 1994; López-Sánchez et al., 1996). The fecal sterol coprostanol was not detected, even though it was a target SIM analyte. The even carbon-number C_{16}-C_{22} *n*-alkylnitriles [37, 45, 54, 60] are indicative of the presence of bacterial organic matter (Sicre et al., 1994), which may, at least in part, be associated with sewage. Alkylnitriles have been documented in the pyrolysis products of sewage sludge (Barrio et al., 1996; Faure et al, 2002). The alkylnitriles

Figure 3a. Total ion current pyrogram. Sediment sample 12 (Old Port). Data collected in full scan mode. See Table 2 for peak identifications, except n-alk-1-enes (^), n-alkanes (+), unidentified coeluent (*), and phthalate (X).

Sample 12 (Port Vell, B-552)
Pyrolysis-GC/MS, Full Scan, Total Ion Current

n-Alkane Carbon Number

CL0112_P
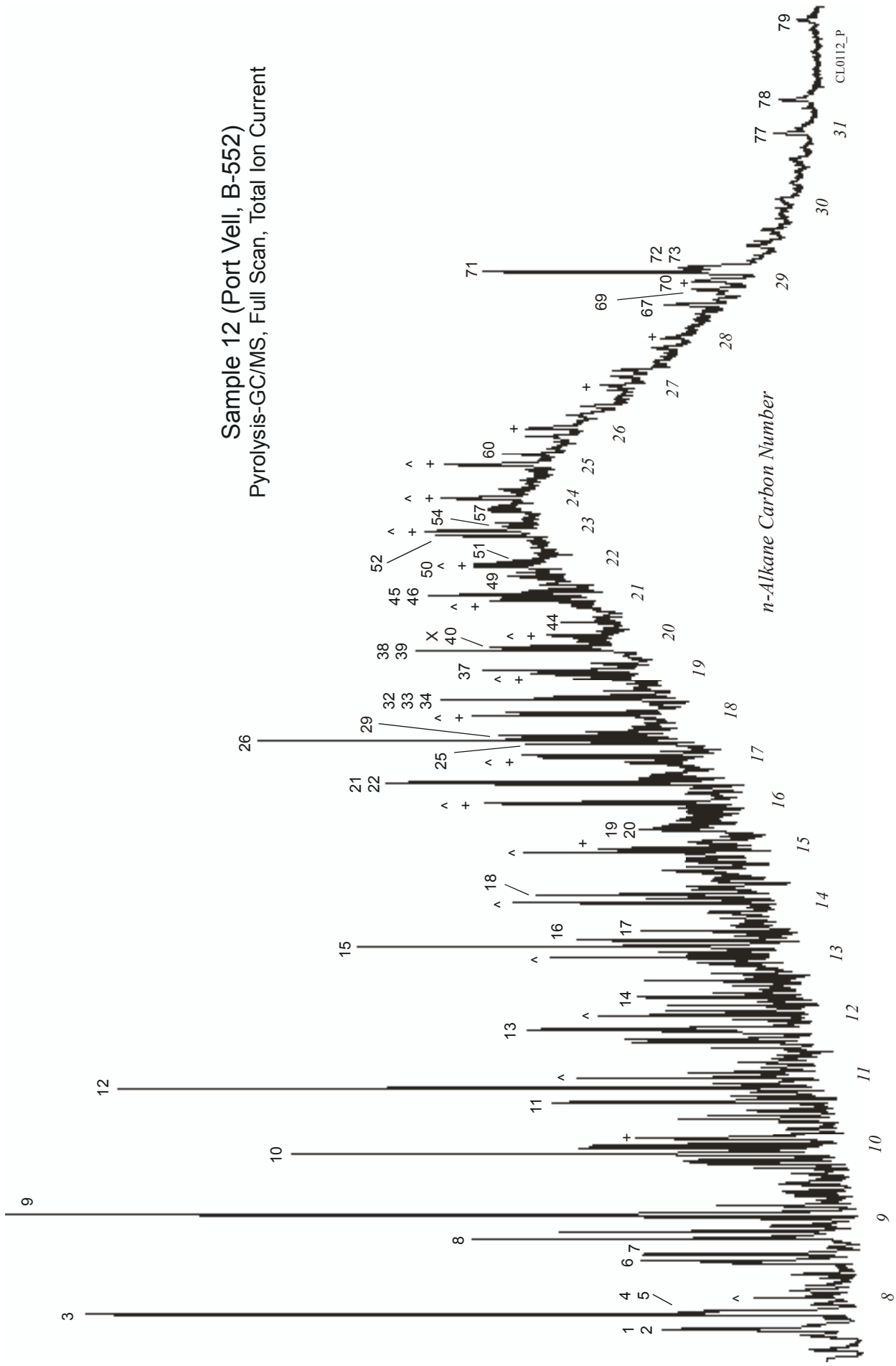
Figure 3b. Total ion current pyrogram. Sediment sample 7 (Port mouth). Data collected in full scan mode. See Table 2 for peak identifications, except n-alk-1-enes (^), n-alkanes (+), unidentified coeluent (*), and phthalate (X).

Sample 7 (Port Mouth, B-547)
Pyrolysis-GC/MS, Full Scan, Total Ion Current

n-Alkane Carbon Number

CL0107_P
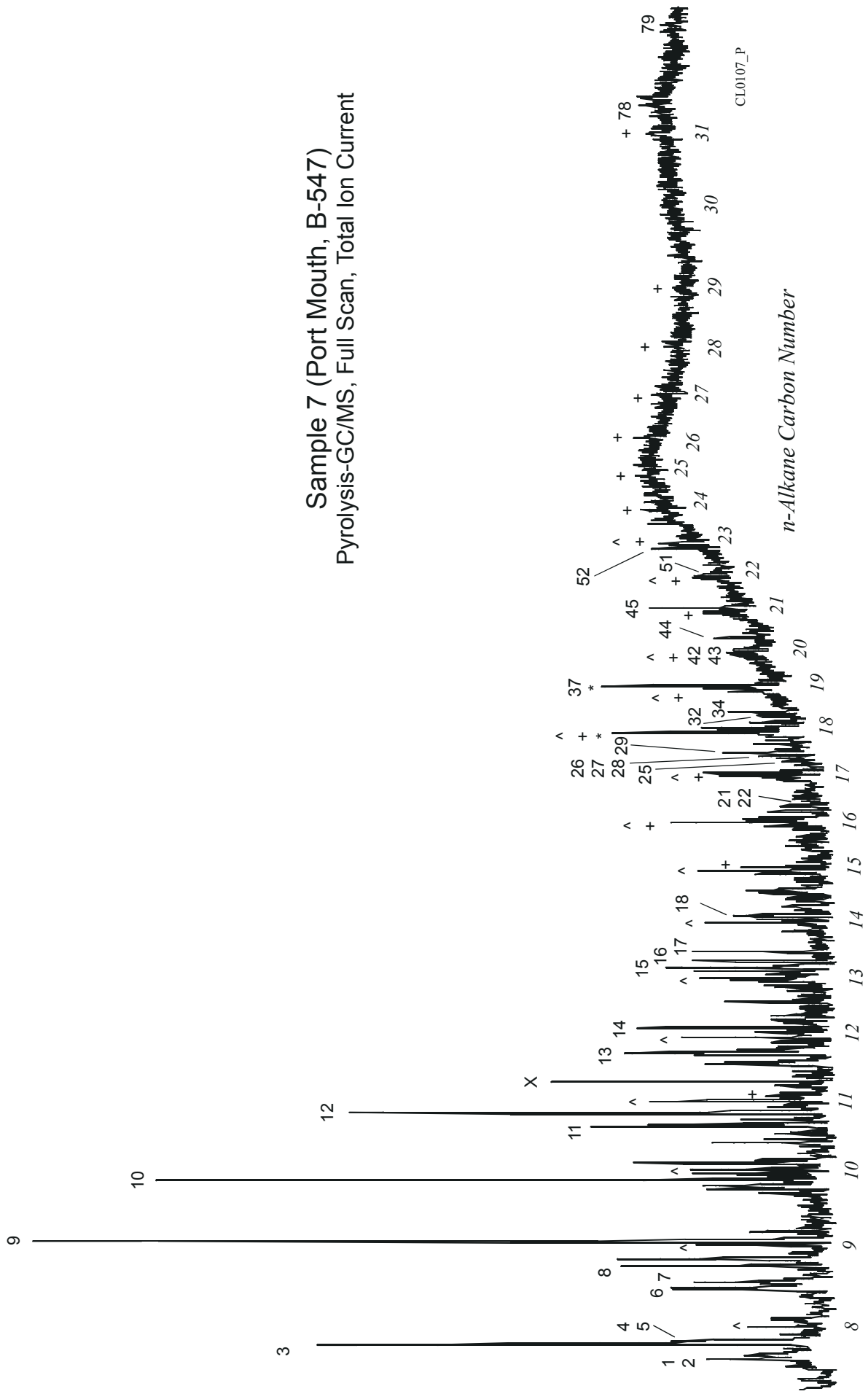
are also visible on the m/z 69+71 mass chromatogram (Fig. 4) along with *n*-hexadecanoic acid [39], another possible marker for bacterial or algal organic matter. The unresolved hump of hydrocarbons, likely due to thermally-desorbed biodegraded petroleum, is clearly in evidence, as are the series of *n*-alkanes and *n*-alk-1-enes, in part likely arising from pyrolytic regeneration from the heavier fractions of biodegraded petroleum (Fig. 4).

A particularly interesting feature of the Old Port sediment pyrolyzate is a prominent series of phenylalkanes (linear alkylbenzenes or LABs) [19-22, 26, 32, 33] clearly visible on the total ion chromatogram (Fig. 3a). The full series is displayed on the m/z 91 mass chromatogram in Figure 5, which shows that the C_{17}-C_{19} phenylalkanes are dominated by their 6-phenyl and 5-phenyl isomers, with secondary amounts of the 4-phenyl. Of the C_{16} phenylalkanes, 5-phenyl- and 4-phenyldecane are detected. Phenylalkanes with these carbon numbers and isomer distributions are environmental markers for common detergents made from linear alkylbenzenesulfonates and are often found in wastewater effluents (Eganhouse et al., 1983; Takada and Ishiwatari, 1987). The isomers with the phenyl substitution towards the interior of the chain, such as those seen in Figure 5, are more resistant to biodegradation than the 2-phenyl and 3-phenyl (Takada and Ishiwatari, 1990), indicating that the detergent residues in the Old Port sediments are at least partly biodegraded. We report here the ability of Py-GC/MS to easily detect detergent-derived phenylalkanes in sediments, mostly likely by thermodesorption.

Polycyclic aromatic hydrocarbons (PAHs) are detectable as relatively minor components in Figure 3a, including phenanthrene, 2-methylphenanthrene, 1,7-dimethylphenanthrene, pyrene and retene [34, 40, 46, 51, 52]. A composite mass chromatogram created using SIM data from pyrolysis of sample 12 presents the full PAH distribution, showing a predominance of parent and methylated phenanthrenes and pyrenes over chrysenes and pentaaromatics (Fig. 6a). The relatively abundant methyl- and dimethylphenanthrenes and methylpyrenes in particular indicate that the PAHs derive primarily from fuel oil, motor oil, diesel and/or crude petroleum. The relatively abundant C_4-alkylnaphthalenes [24] and dibenzothiophene [31] further support this interpretation. The methylated PAHs are of particular concern, as they have been detected in mussels collected in the port area (Baumard et al., 1998). The PAHs detected may have multiple origins. Some are likely to be thermodesorption products (largely analogous to solvent-extractable hydrocarbons) while others may be true pyrolysis products (produced by thermal cleavage of covalent bonds in organic macromolecules). Those (in particular phenanthrene and anthracene) produced in the latter fashion may in fact not arise from sediment pollution, but could be generated by pyrolysis of naturally-occurring lignin and cellulose in the sedimentary organic matter (Sharma and Hajaligol, 2003; McGrath et al., 2003). Companion thermodesorption and solvent extraction analyses would have helped to discriminate between these possible PAH origins, but were not performed during this preliminary study, for which the rapidity of the single, combined thermodesorption/pyrolysis procedure was deemed advantageous.

Figure 4. Summed m/z 69 and 71 mass chromatogram (Py-GC/MS) of sediment sample 12. Data collected in SIM mode. See Table 2 for peak identifications, except n-alk-1-enes (^) and n-alkanes (+).

Distribution of Aliphatics
Sample 12 (Port Vell, B-552)
Py-GC/MS SIM, m/z 69+71

n-Alk-1-ene and n-Alkane Carbon Number

CL0112_Y
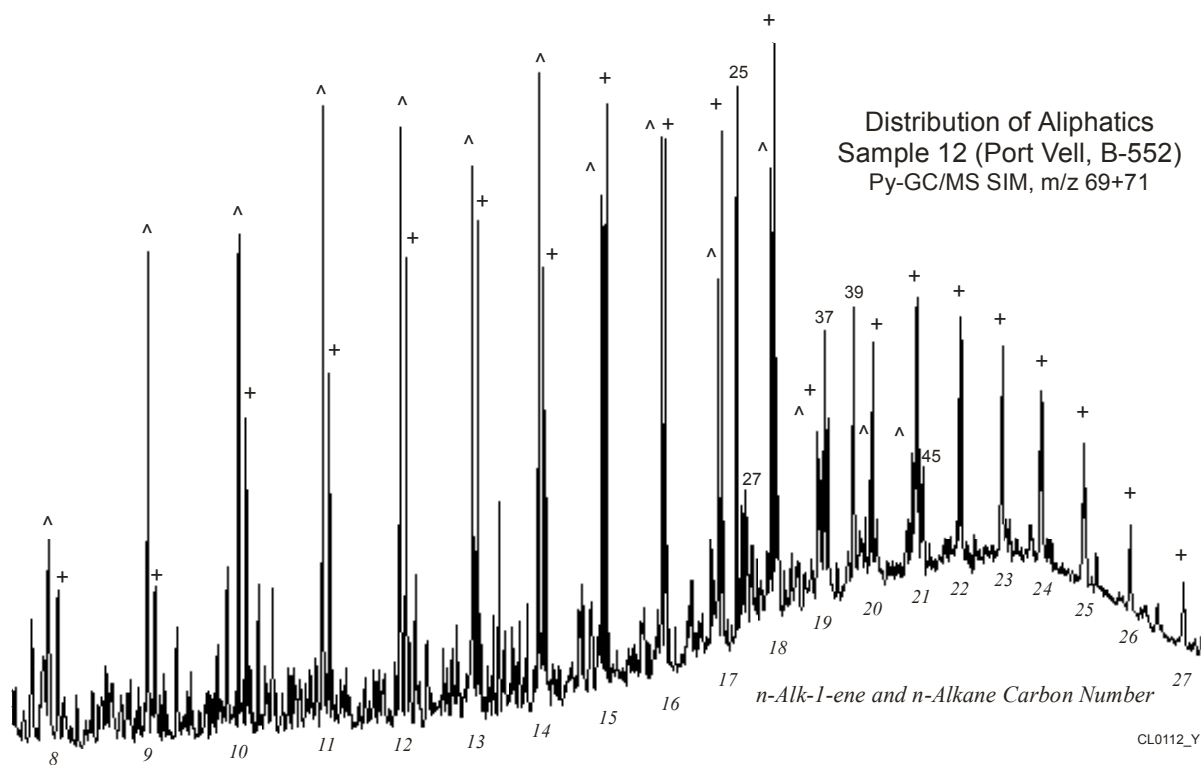
Figure 5. Mass chromatogram (m/z 91, Py-GC/MS, SIM) showing the distribution of C16-C19 phenylalkanes in the pyrolyzate of sample 12 (Old Port). See Table 2 for peak identifications.

Distribution of Phenylalkanes
Sample 12 (Port Vell, B-552)
Py-GC/MS SIM, m/z 91

n-Alkane Carbon Number

CL0112_Y
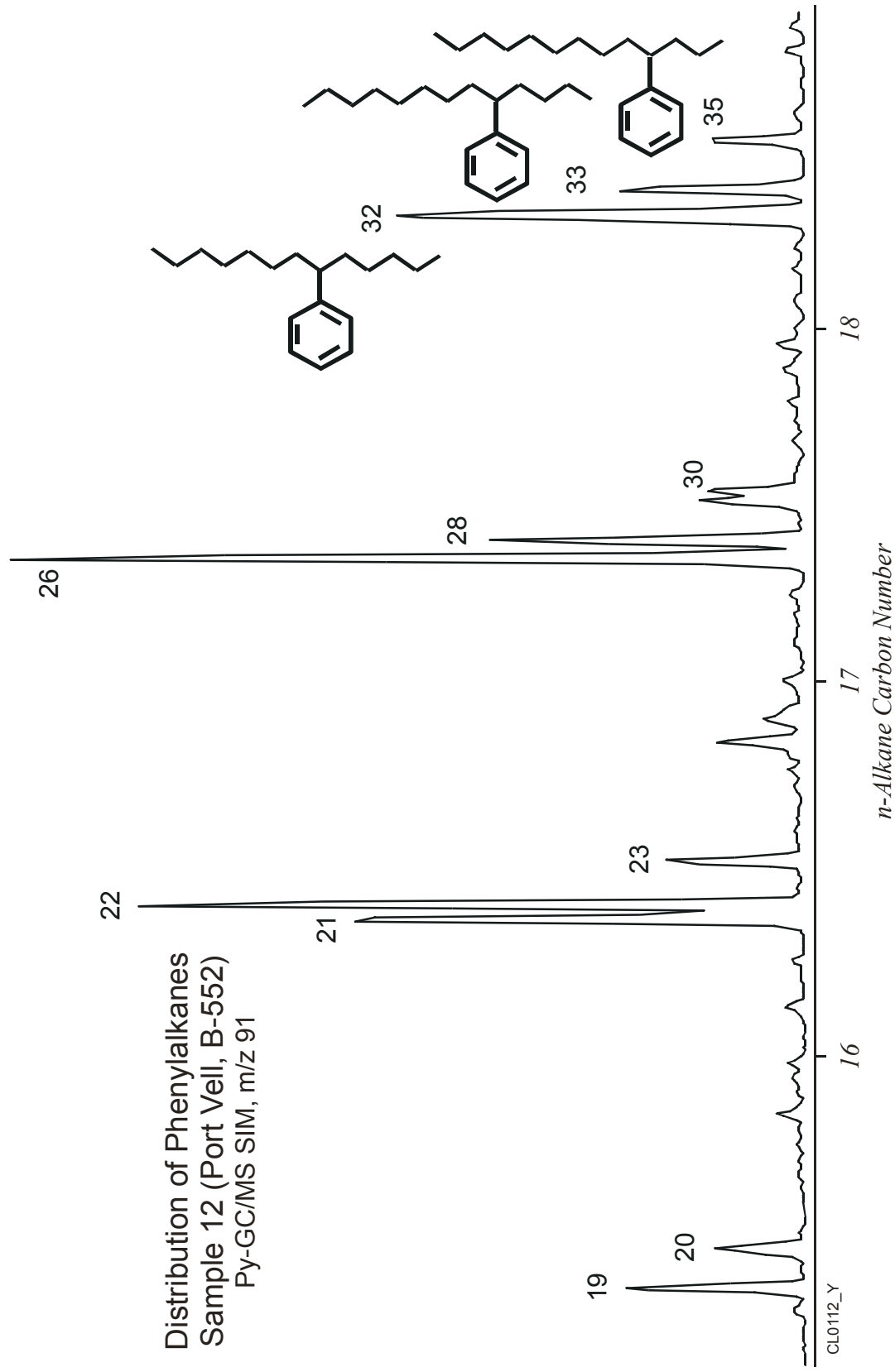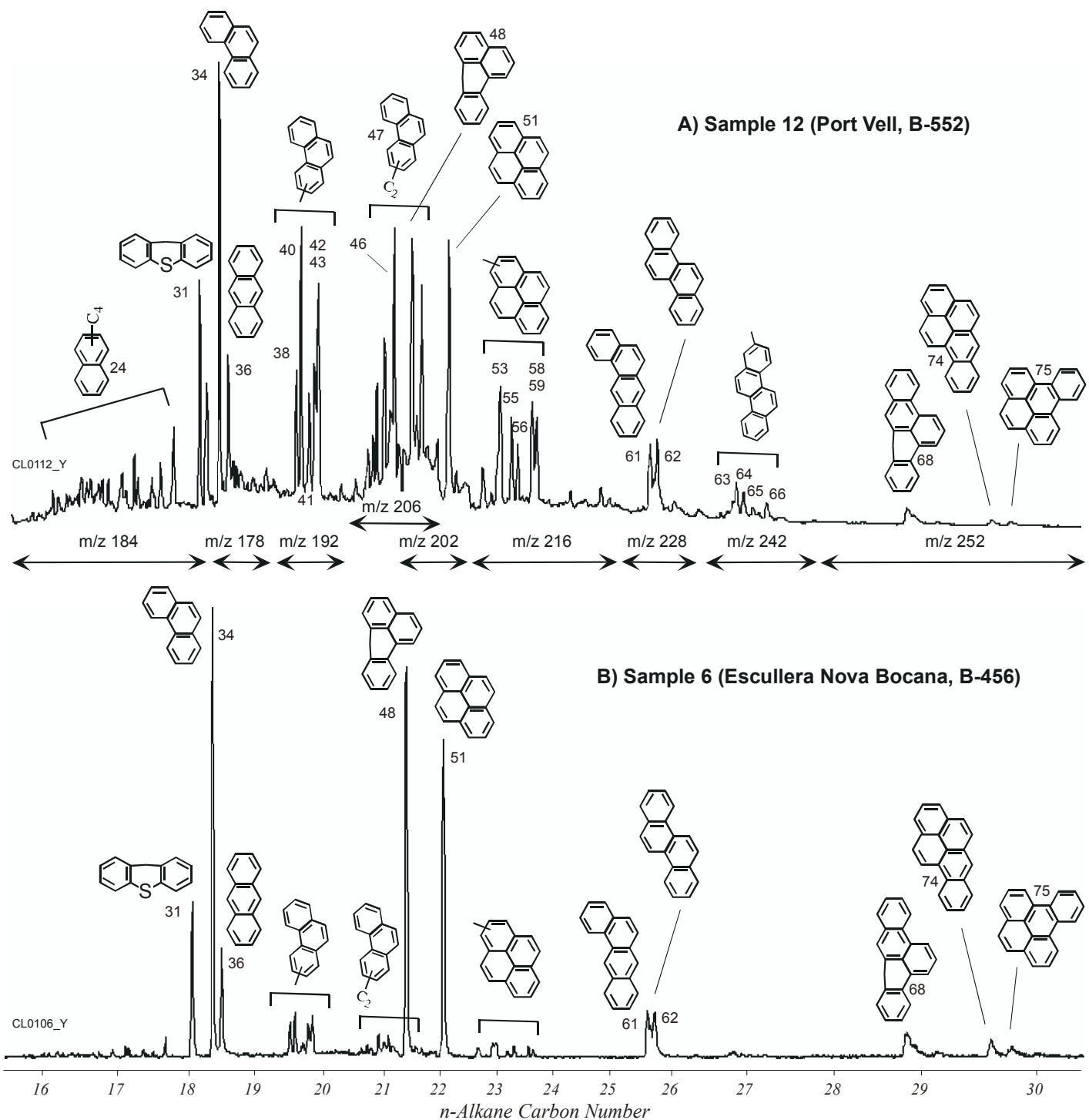
Figure 6. Composite mass chromatograms showing the distribution of PAHs in the pyrolyzates of a) sample 12 (Old Port) and b) sample 6 (outside the breakwater near the site of the proposed new port entrance). Data collected in SIM mode. See Table 2 for peak identifications.

3.2. Consideration of the full sample set

3.2.1. Principal components analysis

With 99 organic compounds quantitated from the SIM Py-GC/MS data and 23 elements, a total of 122 variables, principal components analysis provides a convenient vehicle for data exploration. The resulting first and second principal components accounted for 30 % and 17 % of the variance in the data set, respectively. Examination of the corresponding eigenvectors showed that similar variables (e.g., the phenylalkanes) had similar values. Thus it was possible to combine many variables, leading to an overall reduction to 26 organic compounds and groups of compounds and 8 elements and groups thereof , as described in the methods section (Table 3). The principal components experiment which resulted yielded first and second principal components accounting for 36 % and 21 % of the variance, respectively. The distribution by sample (Fig. 7) is essentially the same as it was in the first experiment with the full 122 variable data set.

Sample 12 and its replicate 12B are clearly distinctive (Fig. 7). The eigenvectors point to strong contributions from the following variables: organic carbon, sulfur, transition metals, hopanes, sterenes, dimethylphenanthrenes and phenylalkanes (Table 3), together indicating petroleum, detergent, industrial and sewage pollution. Phenylalkanes, sterenes and hopanes are readily apparent on the pyrogram of sample 12 (Fig. 3a) but not on the pyrogram of the less contaminated sediment sample 7 (Fig. 3b).   Sample 6 is also distinctive, marked by contributions of combustion-derived parent PAHs. This is also readily evident from its composite mass chromatogram showing the distribution of PAHs (Fig. 6b). Sample 5 has evidently been impacted by petroleum products and metals, as well as combustion products. Samples 1, 2 and 9 show the least affinity for any of the inorganic or organic pollutant variables and thus appear relatively uncontaminated. The remaining samples exhibit intermediate levels of contamination.

3.2.2. Placing the geochemical results in their spatial context

To better appreciate the complex distribution of contaminants in the study area, it is useful to view the geochemical results in their geographical context. Figure 8 provides such a perspective by plotting several of the key geochemical parameters suggested by the principal components analysis. Plotting the first principal component in this way effectively summarizes much of the major contaminant distribution, as it is sensitive to co-occurring trace metals, petroleum, sewage and detergents (Table 3). It achieves its maximum value at sample site 12, in the restricted basin formed by the inner harbor of the Old Port (Figs. 8a, k). Sample site 8, near the automobile and LNG terminals, and site 10, at the inner breakwater (*contradic*), are also impacted by these contaminants, as is sample site 7, at the mouth of the port. Outside the harbor, seaward of the main breakwater, sample site 5 is similarly affected, as are sites 3 and 4, near a major urban/industrial sewage treatment plant outfall at the mouth of the Llobregat River. Within the port sites 9 (container terminal) and 11 (between the Ponent and Barcelona wharves) appear anomalously free of these contaminants, as does site 6, outside the breakwater 1150 m north of site 5. Sites 1 and 2, south of the Llobregat mouth, also appear to be less affected and are evidently sufficiently far from most major sources of contamination.

Figure 7. Plot of the first two principal components produced from the sediment molecular and elemental data using 34 variables (Table 3), as described in the Methods section. The first principal component accounts for 36 % of the variance and the second, for 21 %. The placement, direction and labels of the arrows were determined by examination of the associated eigenvectors.
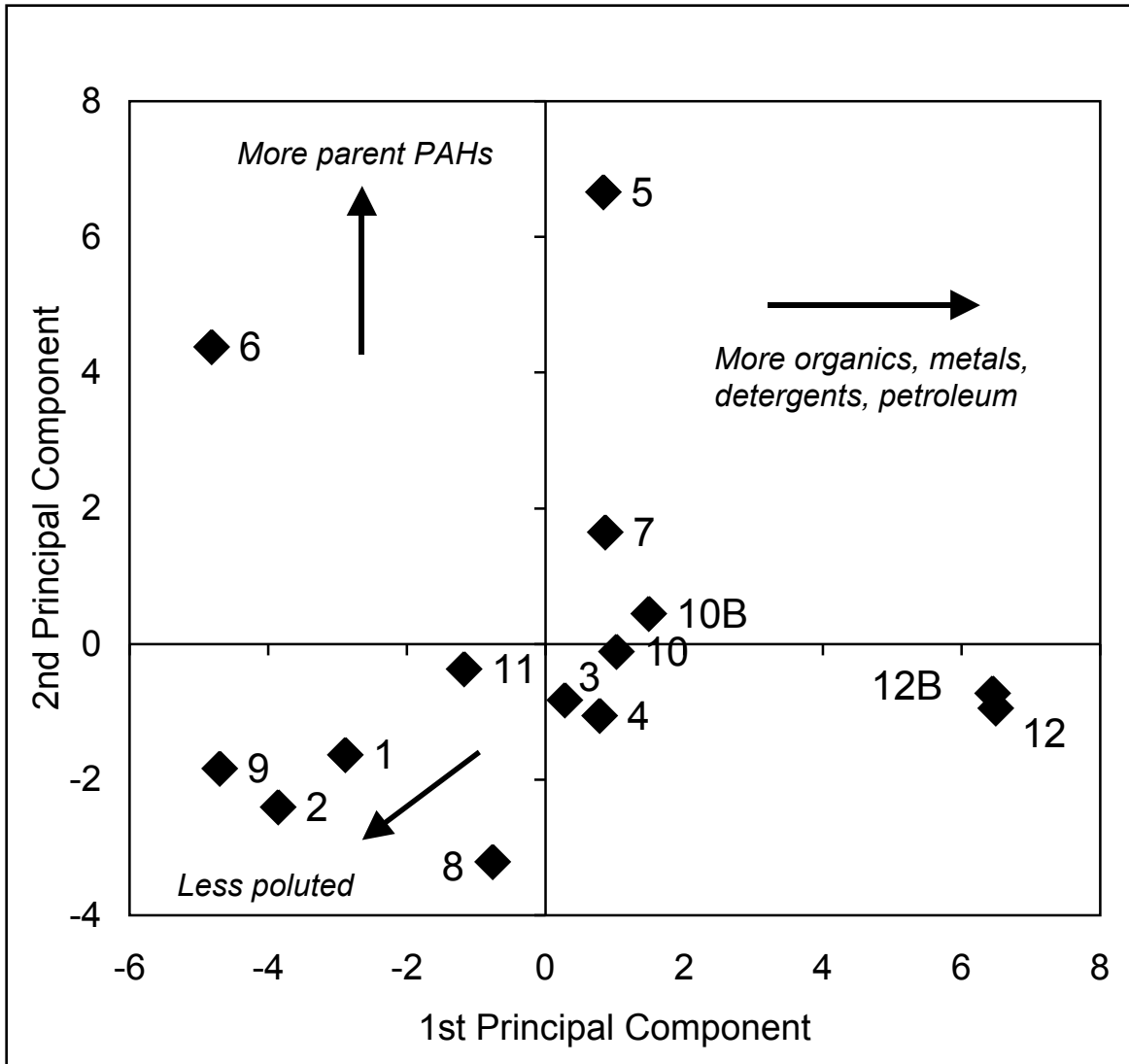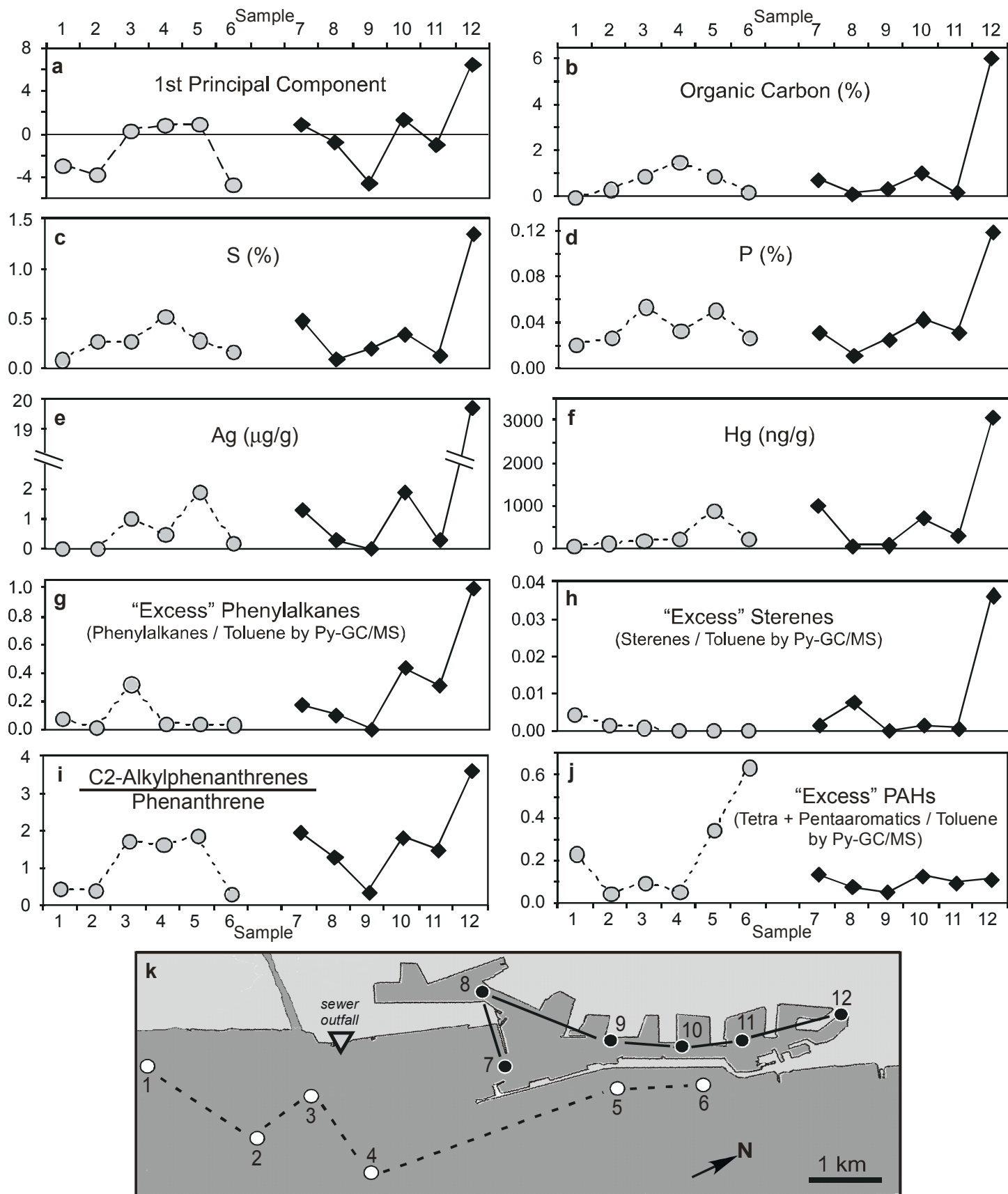
Figure 8. Plots of geochemical parameters for sediments of the offshore transect (sampling sites marked with open circles connected by dashed lines) and the port transect (sampling sites marked by solid circles connected by solid lines). a: first principal component, b: organic carbon, c: sulfur, d: phosphorus, e: silver, f: mercury, g: excess C16-C19 phenylalkanes in the pyrolyzate (see method section for explanation of ratio), h: excess C27 + C29 sterenes in the pyrolyzate (see method section for explanation of ratio), i: ratio of C2-alkylphenanthrenes to phenanthrene determined by Py-GC/MS, j: excess tetra- and pentaaromatic hydrocarbons in the pyrolyzate (see method section for explanation of ratio), k: location map of the Barcelona port and Llobregat River area showing sampling transects; triangle marks a major sewage treatment plant outfall north of the mouth of the Llobregat.

It is also instructive to examine the spatial distribution of individual geochemical variables, of which organic carbon is one of the most significant (Fig. 8b). Its distribution echoes that of the first principal component (Fig. 8a), showing a maximum of 6 % at heavily contaminated site 12, compatible with the occurrence of local hypoxia in the restricted harbor basin. Elevated organic carbon concentrations of about 1 % are present at impacted sites 7 and 10 within the port, site 5 outside and sites 3 and 4 by the river mouth. The port sites 8, 9 and 11, external site 6 and offshore sites 1 and 2 all have low organic carbon contents, between 0.01 and 0.37 % (Fig. 8b, Table 1). The distribution patterns of sulfur and phosphorus closely parallel that of organic carbon, with maxima at site 12 (Figs. 8c, d), again, perhaps evidence of a history of local hypoxic events.

Background silver concentrations near 0 μg/g are recorded in the sediments at offshore sites 1, 2, 6 and at port sites 8, 9 and 11 (Fig. 8e). Similar to the C_{org}, S and P cases, site 12 is the most contaminated (ca. 19 μg/g), while sites 3, 5, 7 and 10 (1-2 μg/g) are less affected. Silver is released into the environment by the photographic, electronic and other industries and is a good tracer for anthropogenic activities due to its typically low natural background levels. Sediment concentrations of other transition metals (Cu, Pb, Zn) show analogous spatial distributions. The distribution of mercury in the sediments follows a similar pattern, with a high of 3 μg/g in the Old Port sediments, except that the sediments at the mouth of the Llobregat are relatively less contaminated. Mercury pollution appears to be more of a concern in the port area, based on this limited set of 12 samples.

The semiquantitative Py-GC/MS results are presented here normalized to pyrolytic toluene (see methods section) and may thus be considered to represent geochemically anomalous or "excess" quantities. The spatial plot for "excess" C_{16}-C_{19} phenylalkanes follows the familiar pattern, reaching its maximum at site 12 and secondary maxima at site 10 within the port and site 3 near the sewage treatment plant outfall at the mouth of the river (Figs. 8g, k). Unlike C_{org}, S, Ag and Hg, the phenylalkanes appear to be a significant factor at site 11. Evidently, detergent laden wastewater causes accumulations of these contaminants in the inner port area and also reaches the coastal waters via the river. The "excess" sterenes are most significant at site 12 (Fig. 8h), marking the locus of the most serious sewage contamination indicated by the sample set.

The "excess" tetra- and pentaaromatic hydrocarbons are most notable in pyrolyzates of sediments from sites 5 and 6, outside the breakwater (Fig. 8j). These samples were also distinctive in having the highest positive values of the second principal component (Fig. 7). Thus these samples are marked by the signature of airfall combustion residues, likely from the ships which anchor at that location while awaiting their turn to enter the port, as well as from ships in the port and the city itself. The dominance of parent compounds in the site 6 PAH distribution strongly contrasts with the relatively abundant alkylated PAHs at site 12 (Fig. 6). The C_2-alkylphenanthrene to phenanthrene ratio is based on this phenomenon and is indicative of petroleum contamination. Its spatial distribution closely parallels that of the first principal component (Figs. 8i and 8a) and is similar to that of sulfur, silver and the phenylalkanes. It indicates a petroleum signature for sediments at sites 3, 4, 5, 7, 8, 10, 11 and (in particular) 12.

It is clearly evident that the site most severely impacted by inorganic and organic pollution is 12, in the restricted basin of the Old Port. Other sites impacted by urban and industrial contaminant deposits with the port area, but to a lesser degree than sampling site 12, are sites 7 and 10 (Table 4). One means by which contaminants likely reached these sites is via the 14 combined sewer overflows distributed along the length of the port. Port records indicate that sites 8, 9 and 11 were dredged to permit access by large ships. Site 9 in particular was dredged most recently, to accommodate container vessels. This explains the consistent lack of pollution observed for sample 9 (Fig. 8) and the absence of at least some of the pollutants in samples 8 and 11. Dredged materials from the port were dumped at site 5, outside the breakwater, explaining its elevated pollutant levels. Site 6 is impacted by airfall combustion debris, likely from ships at least in part, as is site 5, in addition to its burden of dredged materials. The pollution at the mouth of the port (site 7) is more difficult to explain, particularly in the absence of tidal or major fluvial sediment transport. Its contaminants show greater similarity to those of the port than to those discharged by the sewage treatment plant outfall at Llobregat River mouth and evidently deposited at sites 3 and 4 (Fig. 8). Sites 1, in particular, and 2 show little evidence for deposition of contaminants, consistent with their location furthest from the urban center (Fig. 1).

The results of this preliminary survey are encouraging. Future work should continue with a denser sampling program and the development of a geographic information systems approach for the visualization of the resulting large geochemical data in its spatial context. The rapid Py-GC/MS analytical approach would be well-suited to process the large number of samples collected in an expanded program.

4. Conclusions

Enrichment in Corg, S and P was observed at affected sites, as were heavy metal pollutants (Ag, Hg, Pb, Cu, Zn). Evidence for organic pollution included C_{16}-C_{19} phenylalkanes (detergents), hopanes and alkylated PAHs (petroleum), sterenes and alkylnitriles (suspected sewage pollution), and parent PAHs (combustion products). Modes of contaminant transport are sewer outfall (sewage and urban/industrial runoff), aeolian deposition of combustion particulate matter (industrial, vehicular, maritime), removal of polluted sediments by navigational dredging, and dumping of dredged materials. The restricted basin formed by the breakwater in the Old Port is a significant sink for pollutants and is likely the site of episodic water column hypoxia.

This preliminary study demonstrates that Py-GC/MS is effective for rapid screening for organic contaminants in sediments and is in the spirit of "green chemistry", in that it is a microanalytical technique which requires no hazardous solvents. Full-scan MS is recommended for the initial evaluation of a suite of samples, while selected ion monitoring is best for routine detection of trace contaminants. The semi-quantitative data which result are amenable to interpretation using multivariate methods and, with a larger sample set, geographic information systems (GIS), with the potential to provide valuable information for government, industry and public interest groups.

Table 4. Summary of the dominant pollutant types and modes of pollutant transport at the sampling sites.

Site	Location	Transport of pollutants
1	Llobregat delta	Non-deposition
2	Llobregat delta	Minor deposition
3	Llobregat R.mouth (proximal)	Sewer outfall (major); also fluvial
4	Llobregat R. mouth (distal)	Sewer outfall (major); also fluvial
5	Breakwater (Moll Conten.)	Dumping of dredge spoils; Air-fall combustion products
6	Breakwater (new port mouth)	Air-fall combustion products
7	Port mouth	Urban / industrial deposition
8	Fuels dock	Removal by dredging
9	Container dock	Removal by dredging
10	Inner breakwater	Urban / industrial deposition
11	Moll Ponent-Moll Barcelona	Removal by dredging
12	Old Port (Port Vell)	Major urban / industrial deposition

Table 4

Acknowledgements

References

Abdel Bagi S. T., Kruge M. A. and Salmon G. L., 1996. Flash pyrolysis of anthropogenic and natural organic matter in polluted sediments. Preprints of Papers Presented at the 212th ACS National Meeting, 36 (2), 247-249, American Chemical Society Division of Environmental Chemistry.

Barrio M.E., Lliberia J.Ll., Comellas L. and Broto-Puig F., 1996. Pyrolysis-gas chromatography applied to the study of organic matter evolution in sewage sludge-amended soils using nitrogen-phosphorus, flame ionization and mass spectrometric detection. Journal of Chromatography A 719, 131-139.

Baumard P., Budzinski H., Michon Q., Garrigues P., Burgeot T. and Bellocq J., 1998. Origin and bioavailability of PAHs in the Mediterranean Sea from mussel and sediment records. Estuarine, Coastal and Shelf Science 47, 77–90.

Deshmukh A.P., Chefetz B. and Hatcher P.G., 2001. Characterization of organic matter in pristine and contaminated coastal marine sediments using solid-state ^{13}C NMR, pyrolytic and themochemolytic methods: A case study in the San Diego harbor area. Chemosphere 45, 1007-1022.

Eganhouse R.P., Blumfield D.L. and Kaplan I.R., 1983. Long-chain alkylbenzenes as molecular tracers of domestic wastes in the marine environment. Environmental Science and Technology 17, 523-530.

Faure P., Vilmin F., Michels R., Jardé E., Mansuy L., Elie M. and Landais P., 2002. Application of thermodesorption and pyrolysis-GC–AED to the analysis of river sediments and sewage sludges for environmental purpose. Journal of Analytical and Applied Pyrolysis 62, 297–318.

Garcette-Lepecq A., Derenne S., Largeau C., Bouloubassi I. And Saliot A., 2000. Origin and formation pathways of kerogen-like organic matter in recent sediments off the Danube delta (northwestern Black Sea). Organic Geochemistry 31, 1663-1683.

Jardé E., Mansuy L. and Faure P., 2003. Characterization of the macromolecular organic content of sewage sludges by thermally assisted hydrolysis and methylation-gas chromatography-mass spectrometer (THM-GC/MS). Journal of Analytical and Applied Pyrolysis 68-69, 331-350.

Kruge M. A., Mukhophadyay P. K. and Lewis C. F. M., 1998. A molecular evaluation of contaminants and natural organic matter in surface sediments from western Lake Ontario. Organic Geochemistry 29, 1797-1812.

Kruge M. A., 1999. Molecular organic geochemistry of New York Bight sediments. Sources of biogenic organic matter and polycyclic aromatic hydrocarbons. Northeastern Geology and Environmental Sciences 21, 121-128.

López-Sánchez J.F., Rubio R., Samitier C. and Rauret G., 1996. Trace metal partitioning in marine sediments and sludges deposited of the coast of Barcelona (Spain). Water Resources 30, 153-159.

Mansuy, L., Bourezgui, Y., Garnier-Zarli, E., Jardé, E., Réveillé , V., 2001. Characterization of humic substances in highly polluted river sediments by pyrolysis methylation-gas chromatography-mass spectrometry. Organic Geochemistry 32, 223–231.

McGrath T.E., Chan W.G. and Hajaligol M.R., 2003. Low temperature mechanism for the formation of polycyclic aromatic hydrocarbons from the pyrolysis of cellulose. Journal of Analytical and Applied Pyrolysis 66, 51-70.

Palenques A., 1994. Distribution and heavy metal pollution of the suspended particulate matter on the Barcelona continental shelf (North-Western Mediterranean). Environmental Pollution 85, 205-215.

Palenques A. and Diaz J.I., 1994. Anthropogenic heavy metal pollution in the sediments of the Barcelona continental shelf (Northwestern Mediterranean). Marine Environmental Research 38, 17-31.

Peters K.E. and Moldowan J.M., 1992. The Biomarkers Guide: Interpreting Molecular Fossils in Petroleum and Ancient Sediments. Prentice Hall, 352 p.

Peulvé S., de Leeuw J.W., Sicre M.-A., Bass M. and Saliot A., 1996. Characterization of macromolecular organic matter in sediment traps from the northwestern Mediterranean sea. Geochimica et Cosmochimica Acta, 60: 1239-1259.

Richnow H.H., Seifert R., Kästner M., Mahro B., Horsfield B., Tiedgen U., Böhm S. and Michaelis W., 1995. Rapid screening of PAH-residues in bioremediated soils. Chemosphere 31, 3991-3999.

Rushdi A.I., Ritter G., Grimalt J.O. and Simoneit B.R.T., 2003. Hydrous pyrolysis of cholesterol under various conditions. Organic Geochemistry 34, 799-812.

Sharma R.K. and Hajaligol M.R., 2003. Effect of pyrolysis conditions on the formation of polycyclic aromatic hydrocarbons (PAHs) from polyphenolic compounds. Journal of Analytical and Applied Pyrolysis 66, 123-144.

Sicre M.-A., Peulve S., Saliot A., de Leeuw J. W. and Baas M., 1994. Molecular characterization of the organic fraction of suspended matter in the surface waters and bottom nepheloid layer of the Rhone delta using analytical pyrolysis. Geochimica et Cosmochimica Acta 21, 11-26.

Takada H. and Ishiwatari R., 1987. Linear alkylbenzenes in urban riverine environments in Tokyo: Distribution, Source and Behavior. Environmental Science and Technology 21, 875-883.

Takada H. and Ishiwatari R., 1990. Biodegradation experiments of linear alkylbenzenes (LABs): Isomeric composition of C_{12} LABs as an indicator of the degree of LAB degradation in the aquatic environment. Environmental Science and Technology 24, 86-91.

U.S.E.P.A., 1996. Semivolatile organic compounds (PAHs and PCBs) in soils/sludges and solid wastes using thermal extraction/gas chromatography/mass spectrometry

(TE/GC/MS). United States Environmental Protection Agency Method 8275A, Revision 1.

Zang X. and Hatcher P.G., 2002. A Py-GC-MS and NMR spectroscopy study of organic nitrogen in Mangrove Lake sediments. Organic Geochemistry 33, 201–211.